

A Novel Approach for Abnormality Detection of Macula and Fovea Region from Color Fundus Images

Shobhana.M and S.B.Chitrapreyanka

Abstract: The macula is the central portion of the retina, a small region rich in cones, the particular nerve endings that detect the color and upon which daytime vision depends. The macula is responsible for clear central vision. The remaining part of the retina is used for side or peripheral vision. The fovea centralis, usually known as the fovea, is located in the center of the macula region on the retina. The fovea is responsible for sharp central vision and is the most important part of the retina for human vision. Macular edema is often a complication of diabetic retinopathy and is the most common form of vision loss for people with diabetes particularly if it is left untreated. In this paper, a two stage methodology is employed to detect the macular edema and a simple, fast algorithm using mathematical morphology is employed to find the fovea region. An automatic disease detection system can significantly reduce the load of experts by limiting the referrals to those cases that require immediate consideration. The reduction in time and effort will be significant where a majority of patients screened for diseases turn out to be normal. Such a solution will be a value addition to the existing infrastructure of Diabetic Retinopathy (DR) screening.

Keywords: Abnormality detection, Diabetic Retinopathy, Fovea, Hard Exudates, Macular Edema.

I. INTRODUCTION

Diabetic Macular Edema (DME) is caused by leaking macular capillaries. There are many causes of macular edema. It is often associated with diabetes, where broken blood vessels in the retina begin to leak fluids, containing small amount of blood, into the retina. At times deposits of fats may leak in to the retina. This leakage causes swelling in the macula region. Eye surgery, comprising cataract surgery, can increase the risk of developing macular edema due to blood vessels becoming irritated and leaking fluids. Macular edema that matures after cataract surgery is called Cystoid Macular Edema (CME).

Some of the other macular edema causes includes age-related macular degeneration, uveitis, retinal vein occlusion. Macular edema is often painless and may display few symptoms when it advances. When symptoms do follow, they are a sign that the blood vessels in the eye may be leaking. Symptoms of macular edema may include blurred or wavy central vision and/or colors appear washed out or changed. If left untreated, macular edema can cause severe vision loss and even blindness.

Macular edema occurs when fluid and protein deposits collect on or under the macula of the eye (a yellow central area of the retina) causing it to thicken and swell. The swelling may damage one's central vision, as the macula is present near the center of the retina at the back of the eyeball. Diabetic macular edema is mainly classified into focal and diffuse types. Focal macular edema which tends to leakage fluid is caused by foci of vascular abnormalities, primarily micro aneurysms, whereas diffuse macular edema is caused by dilated retinal capillaries in the retina [1], [2]. Two types of laser treatment for diabetic macular edema are focal and grid. The aim of focal laser treatment is to treat focal diabetic macular edema and to close leaking micro aneurysms. Similarly, the aim of grid laser treatment is to treat diffuse diabetic macular edema and is applied to areas of retinal thickening in which there is diffuse leakage to produce a retinal burn of mild to moderate intensity.

Diabetic Retinopathy is a complication of the retina due to diabetes and is a leading cause of blindness in urban population. Among the most serious DR abnormalities, hard exudates should be detected and treated immediately to prevent vision loss. Hard exudates occur in retina due to vascular debilities caused from prolonged diabetes. They are normally represented by bright yellowish lesions of different sizes and brightness. The location and extent of these lesions determine the resulting severity of diabetic retinopathy. Hard exudates are abnormal lesions caused by diabetic retinopathy in a diabetic's eye. They are considered to be one of the bright intensity regions in the retinal images and appear as random yellowish patches. The size and distribution of exudates may vary during the progress of the disease.

DME is generally detected directly or indirectly. Direct ways are using stereoscopy or optical computed tomography images [3]. Indirect method is by detecting the presence of hard exudates (HE) in the retina. HE is formed due to secretion of plasma from capillaries resulting from the

Shobhana.M is M.E student, Applied Electronics, K.S.R. College of Engineering, Tiruchengode and S.B.Chitrapreyanka is working as Assistant Professor, Department of EEE, K.S.R College of Engineering, Tiruchengode
Emails: shobhamohan69@yahoo.com, cp_priy@yahoo.com

complications of retinal vasculature and could lead to retinal swelling [5]. In color fundus images they appear as yellow–white deposits.

Fovea is the most important part of the retina for human vision. If the delicate cones of our fovea are destroyed, the person turns out to be blind. The size of fovea region in fundus image of the eye has relation with various diseases, which may lead to blindness. Usually the zone is approximated to a circle of radius 200micron [1]. If the said radius is smaller then, we can conclude that there may be some deposition at the peripheral side, and that causes some infection or disease in eye, which may tend to retinopathy or blindness. Also the radius of the fovea region may indicate the stages of retinopathy [13].

Manual detection of fovea region by ophthalmologists is time consuming. Due to unavailability of trained ophthalmologists especially in developing countries like India, automation is highly needed. Fovea is characterized by the center of the macula. In fundus retinal image the macula is the darkest part approximated by a circle. Geometrically fovea is said to be located at a distance 2.5 times the diameter of the Optic Disk(OD) from its center [2].In this paper, detecting the presence of hard exudates (HE) in macula region is considered a standard method to assess DME from color fundus images. In the next stage, the geometrical distance between OD and fovea region and the structure of the blood vessels is utilized to perfectly localize the fovea region.

II. ALGORITHM FOR DETECTING MACULAR EDEMA

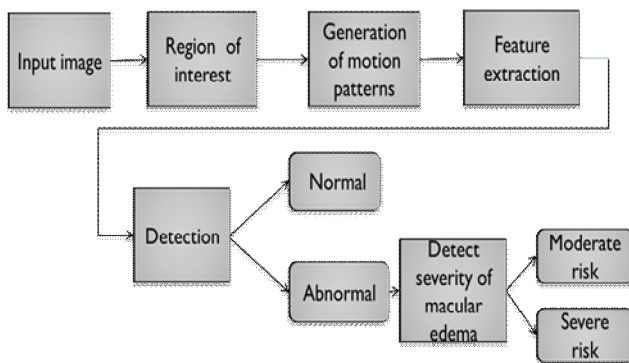


Figure 1: Block Diagram for Detection & assessment of Macular Edema

The macula is a dark structure roughly at the center of the retina. Hard Exudates which appear as clusters of bright lesions are usually well localized. In the absence of any HE (i.e., a normal retina), there is a rough rotational symmetry about the macula in the circular region of roughly twice the diameter of the optic disc.

We use this observation to derive relevant features to describe the normal and abnormal cases. Given a color fundus image, a circular region of interest (ROI) is first extracted and an intermediate representation also known as

the motion pattern of the ROI is created [22]. Relevant features are then derived for to classify the given image as normal or abnormal.

A. Macula Localization (ROI Extraction)

Since the severity of DME is determined based on the location of HE clusters relative to the macula, the images acquired for DME detection usually focus around the macular region. We find the best fit circle within the fundus mask with macula at the center for a given image. The region within this circle is the desired ROI denoted as (see Fig.2 for an example).

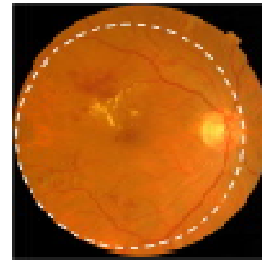


Figure 2: The region of interest centered on macula in a fundus image.

Detection of optic disc: An efficient detection of optic disc in color retinal images is a significant task in an automated retinal image analysis system. Its detection is prerequisite for the segmentation of other normal and pathological features. The position of optic disc can be used as a reference length for measuring distances in retinal images, especially for the location of macula [13]. In case of blood vessel tracking algorithms the location of optic disc becomes the starting point for vessel tracking.

The attributes of optic disc is similar to attributes of hard exudates in terms of color and brightness. Therefore it is located and removed during the hard exudates detection process, thereby avoiding false positives. In color fundus photograph, optic disc appears as a bright spot of circular or elliptical shape, interrupted by the outgoing vessels [8]. It can be seen that optic nerves and vessels emerge into the retina through optic disc. It is situated on the nasal side of the macula and it does not contain any photoreceptor. Therefore it is also called the blind spot.

Localization of Optic Disc: The localization of optic disc is important for two purposes. First, it serves as the baseline for finding the exact boundary of the disc. Secondly, optic disc center and diameter are used to locate the macula in the image [10]. In a color retinal image the optic disc belongs to the brighter parts along with some lesions. The central portion of disc is the brightest region called optic cup, where the blood vessels and nerve fibers are not present. A threshold is to be applied, that will separate part of the optic disc and some other unconnected bright regions from the background.

Elimination of Vessels: The optic disc region is usually fragmented into multiple sub-regions by blood vessels that have comparable gradient values. A homogeneous optic disc region is needed for segmentation using geometric active

contour algorithm. Median filter with appropriate size is used to remove interfering blood vessels from the optic disc region resulted in heavy blurring of disc boundaries [5]. Instead a better result is achieved with gray level mathematical morphology to remove irrelevant vessels from the optic disc region.

Gray scale mathematical morphology provides a tool for extracting geometric information from gray scale images. A structuring element is used to build an image operator whose output depends on whether or not this element fits inside a given image. Shape and size of the structuring element is chosen in accordance with the segmentation task. The two fundamental morphological operations are dilation and erosion [5]. Due to dilation operation the small interfering blood vessels are detached. Next, erosion is done to restore the boundaries to their former position.

Detection of Macula: The macula is a depression in the center of macular region and appears as a darker area in a color retinal image. It is located temporal to the optic disc and has no blood vessels present in its center.

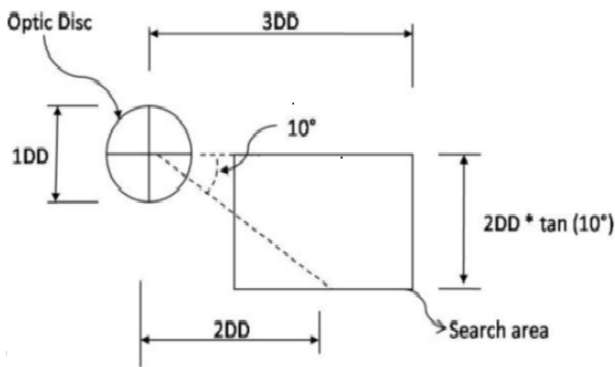


Figure 3: Illustration of finding a search area to localize macula.

Since the location of macula varies from individual to individual, a rectangular search area has to be defined. In a standard retinal image the macula is situated about 2 disc diameter (DD) temporal to the optic disc [17], [18]. Based on this prior knowledge a rectangular search area is formed as shown in Fig.3. The width of the search area is taken equal to two Disc Diameter (2DD) as the mean angle between the macula and the center of the optic disc to the horizontal. A small pixel window of size 40×40 is formed to scan the entire area and the average intensity at each pixel location is calculated. The center of the window having the lowest average intensity is taken as the center of the macula. Fig.3 shows the result of automatic macula detection method. As the macula is localized, the whole macular region can be determined for detecting the presence or absence of hard exudates.

B. Combining the Motion Patterns

When an object in a scene moves at a high speed, it usually leaves a smearing pattern in the captured image. Generally, the spatiotemporal changes recorded by the sensor are characteristic of the moving object.

Signal aggregation at sensor locations in human eyes and camera, gives rise to the smearing effect. For simulating this effect, a motion is induced in a given image to generate a sequence of images. These are combined by applying a function to coalesce the intensities at each sensor (or pixel) location (i.e. pixel position across the sequence) to give rise to a motion pattern [19]. Let a region of interest (ROI) in a medical image be denoted as $I(r)$. By inducing motion on image I , a motion pattern I_{MP} is obtained as follows

$$I_{MP}(r) = f(G_N(I(r))) \quad (1)$$

Where r denotes a pixel location, is a transformation representing the induced motion which is assumed to be rigid. G_N generates N transformed images which are combined using f to coalesce the sampled intensities at each pixel location as given in (1). Since, the severity of the disease is directly related to the radial distance of HE in the circular ROI, rotational motion is induced to generate the desired. The transformation function is applied to generate a sequence of images which are rotated versions. The spatial extent of smearing of intensities depends on the maximum rotation whereas the sampling rate at each location is directly related to the size of each rotation step. Consider a disk with a single circle near the periphery modeling a lesion. When rotation is applied to this pattern, a set of patterns are generated. When two patterns will be generated and their union is the second pattern [18], [19]. The remaining patterns are the result of the union of patterns generated with decreasing step size. It can be observed that a decrease in the step size results in several copies of the lesion in the final result. Here, the motion pattern is obtained by using the union operation as the coalescing function.

Accordingly, two functions namely mean and maximum were considered in this work. While the coalescing function mean obtained tries to achieve the averaging effect observed in motion blur, maximum obtained tries to exploit the fact that HE usually appear brighter than any other structures in the background at the same radial distance[6]. The original and motion pattern images illustrate the effect of the two coalescing functions on a normal and two abnormal fundus images

C. Feature Selection

The motion pattern generated by inducing motion on image I , results in the smearing of lesions when present, along the motion path. To effectively describe this motion pattern, we propose to use a descriptor derived from the Radon space [10]. The Radon transform of is the integral of along a line oriented at and distance from the origin.

$$P \propto (r) = \int f(x, y) \delta(r - x \cos \alpha - y \sin \alpha) dx dy \quad (2)$$

Where, α is the angle between the line and y axis.

The image is projected to obtain a vector response for every angle and the desired feature vector then is derived by concatenating the responses for different orientations. The spatial extent of any HE that may be present is enhanced in

the motion pattern and is in turn reflected immediately in the projection based feature vector [12]. Thus, the feature vector for an abnormal retina will have several peaks in its profile due to intensities corresponding to HE. On the other hand, the feature vectors for a normal retina will have relatively uniform values resulting in a compact normal subspace. These feature vectors are used for learning the subspace corresponding to normal images.

D. Abnormality Detection

Single class classifiers are used for learning normal cases. In this approach, a classification boundary is formed in the feature space around the subspace corresponding to normal cases [15]. If a new image is transformed to this feature space, is within this boundary, then it is classified as normal and abnormal elsewhere. Two class classifiers are used in this work are: Gaussian data description (Gaussian DD) and principal component analysis data description (PCA DD).

Gaussian Data Description: Here, the normal class is modeled as a Gaussian distribution. The model parameters, namely, the mean μ and the covariance Σ are computed for the training set made of normal cases. Classification of a new case is based on the Mahalanobis distance between the new case and the normal subspace.

$$D(g(I_{MP})) = (g(I_{MP}) - \mu)^T \Sigma^{-1} (g(I_{MP}) - \mu) \quad (3)$$

Principal Component Analysis: Here, a linear subspace is defined for the normal cases. The eigenvectors corresponding to the covariance matrix of the training set is used to describe the subspace. The feature vector for a new case is projected to this subspace and again reconstructed.

For both the above single class classifiers, the classification between normal and abnormal images is then performed using an empirically determined threshold on and for Gaussian DD and PCA DD classifiers, respectively [8]. Thus far, we have described the methodology for determining if a given image is normal or abnormal.

E. Severity Assessment of Macular Edema

Assessing the severity of macular edema is very important. The macula in a normal image is relatively darker than other regions in the fundus image and is characterized by (rough) rotational symmetry. We use this symmetry information to establish the risk of exhibiting edema [13], [15]. Good degree of symmetry is taken to indicate the abnormality is not inside macula and hence it is declared as a moderate case. Asymmetry of the macula on the other hand implies abnormality is within the macula and hence the case is considered as severe.

A threshold on the symmetry measure S is used for assessing the degree of abnormality of an image as moderate or severe risk of DME [9]. Let S_{max} and S_{min} be the maximum and minimum symmetry values for normal images in the training set used for abnormality detection. Then the severity of a given abnormal image is determined by comparing the

symmetry measure of this image $S(I_a)$ against a threshold T as follows,

$$\text{Severity}(I_a) = \begin{cases} \text{moderate}; & \text{if } S(I_a) \leq T \\ \text{severe}; & \text{otherwise} \end{cases} \quad (4)$$

Threshold T should be selected to be a percentage p of the maximum symmetry value for normal images. Hence, the threshold is selected as

$$T = P(S_{max} - S_{min}) + S_{min} \quad (5)$$

III. ALGORITHM FOR FOVEA EXTRACTION

Input: Gray-scale fundus image ($I1$), an image $I5$ (contains only blood vessels), approximate center (G) and diameter (d) of the optic disk.

Output: Macula and fovea region.

Step 1: Locate a point P horizontally at a distance $2.5 \times d$ from G towards the centroid.

Step 2: A vertical strip of width k pixels is considered around P perpendicular to GP .

Step 3: Apply a $k \times k$ sliding window along the strip and form the chain of numbers denoting the black pixels in the window.

Step 4: Find the maximum run length of zeros, L in the number chain.

Step 5: Let S and E are the start and end position corresponding to L and D be the mid position of S and E .

Step 6: Consider a binary image BW of size same as the input image with only a black pixel at position D . Dilate BW by a disc of radius DS to obtain BWd .

Step 7: Obtain portion of the gray-scale image as $R, I1$ corresponding to the black region in BWd .

Step 8: Binarize the gray scale image to approximate macula region [16].

Step 9: Refine binarized image by removing noise and fitting the circle to obtain final macula region.

Step 10: Fovea region is to be detected as small area around the center of macula. It is marked by a red colored circle.

IV. SIMULATION OUTPUT

The simulation tool used for processing input color fundus images is MATLAB. The version of MATLAB is 7.12. Image processing toolbox is used for simulation. The input contains both normal and abnormal images. The input eye images are in digital format. It is in .jpg format.

A. Conversion to Gray Scale Image

To reduce the correlated color information in color fundus image as shown in Fig 4(a), RGB image is converted into gray-scale as input image as shown in Fig 4(b).

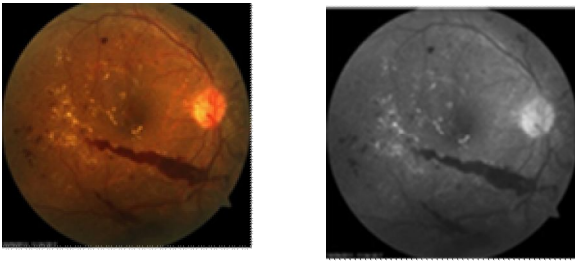


Figure 4: (a) color fundus image (b) gray scale image

B. Morphological Operations on Gray Scale Image

Morphological opening operation and Morphological closing operation are applied to a disk shaped structuring element on gray-scale image to reduce the small noise and to remove the vessels structure as shown in Fig.5(a) and Fig.5(b) respectively.

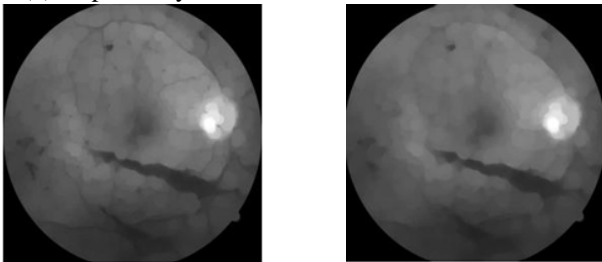


Figure 5: (a) erosion operation (b) dilation operation

Due to dilation operation, the small interfering blood vessels are detached. This will make the input image slightly blurred. Next, erosion is done to restore the boundaries to their former position.

C. Blood Vessel Extraction and Optic Disc Detection

The blood vessels of the disk are found using MATLAB morphological filters. Based on the adaptive mathematical morphology, the origin of the optic disc is identified.

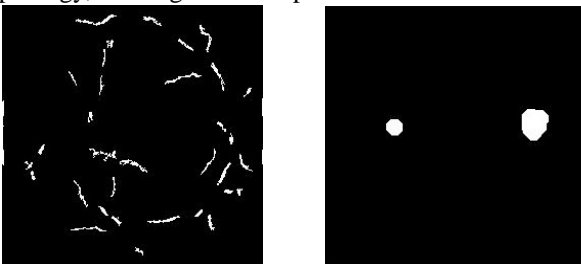


Figure 6: (a) Blood vessel extraction (b) OD detection

The macula, which is a depression in the center of macular region, appears as a darker area in a color retinal image. It is located temporal to the optic disc and has no blood vessels present in it. Blood vessel extraction for the input image (vessel detected image) is shown in Fig.6 (a) and the optic disc detected is shown in Fig.6 (b).

D. Generation of Motion Patterns

When rotation is applied to the disk pattern in steps of $\theta_0 = \pi$, a set of patterns is generated. When two patterns will be generated and their union is the second pattern. The remaining patterns are the result of the union of patterns generated with decreasing step size.

The motion pattern is obtained by using the union

operation as the coalescing function. As shown in Fig.7 similar eight motion patterns are generated in the decreasing rotation steps.

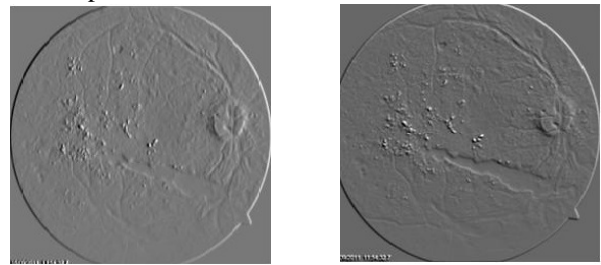


Figure 7: Motion patterns of decreasing rotation steps

E. Combined Motion Patterns and Segmented Image

Combining the eight motion by applying the rotation steps in decreasing order from $(0 \text{ to } 2\pi)$ is obtained as shown in the Fig.8(a) and the segmented image with affected areas are obtained as shown in the Fig.8(b).

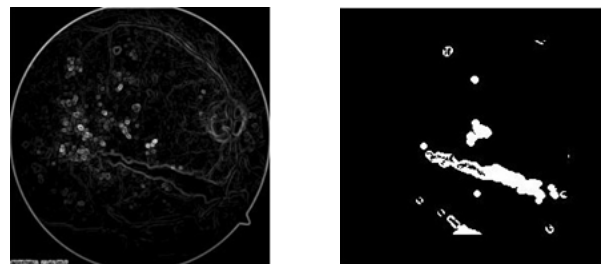


Figure 8:(a) combined motion pattern (b) segmented image

Determining the severity of macular edema is an another task. The macula in a normal image is relatively darker than other regions in the fundus image and is characterized by rotational symmetry. Good degree of symmetry is taken to indicate the abnormality is not present inside macula and hence it is declared as a moderate case. Asymmetry of the macula on the other hand implies abnormality is within the macula and hence the case is severe.

F. Fovea extraction and the image with affected areas

A point is located horizontally at a distance $2.5 \times d$ from optic disk center towards the centroid. A $k \times k$ sliding window is applied along the strip and forms chain of numbers denoting the black pixels in the window.

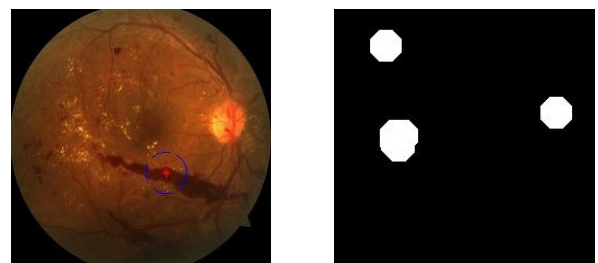


Figure 9: (a) fovea localization (b) affected areas

Maximum run length of zeros is found in the number chain. That is known as a fovea region. It is marked by a red colored circle as shown in fig.9(a) and checking of that image to spot the disease is done by visualizing the change in the

shape of fovea .The affected areas of the retinal image are shown in fig.9(b).

V. RESULTS AND DISCUSSION

The output segmented image for determining the macula edema, that is detecting the presence of hard exudates near the macula region is obtained through different steps in the proposed algorithm. The steps includes region of interest extraction, generation of motion patterns, feature selection, abnormality detection, severity analysis. The following are observed in the command window of MATLAB: the elapsed time, normal or abnormal retina and if it is abnormal, whether it is moderate or severe risk. Then the fovea region is extracted and depending on the change in shape of the fovea, the affected regions are found out.

VI. CONCLUSION

DME detection and assessment provides significant contributions which include a hierarchical approach to the problem, a novel representation for the first level, to classify an image as normal or abnormal (containing HE) and a rotational asymmetry measure for the second level, to assess the severity of DME. This novel representation captures the global image characteristics. Such global features have not been used successfully earlier for HE detection. In the first level, a supervised technique based on learning the image characteristics of only normal patients is used for detecting the abnormal cases pertaining to HE. In the second level, the severity of the abnormality is assessed by analyzing the rotational asymmetry of the macular region in retina. Further in this paper, a new efficient method is described to localize the fovea in retinal fundus image. Morphological operators and geometrical features are used to localize the fovea region successfully. Proposed scheme is simple but efficient in extracting the fovea region. The extracted macula and fovea region may help in further diagnosis of eye related diseases.

REFERENCES

- [1] L. Giancardo, F. Meriaudeau, T. P. Karnowski, Y. Li, K. W. Tobin, Jr., and E. Chaum, "Automatic retina exudates segmentation without a manually labeled training set," in Proc. 2011 IEEE Int. Symp. Biomed. Imag: From Nano to Macro, Mar. 2011, pp. 1396–1400.
- [2] L. Giancardo, F. Meriaudeau, T. Karnowski, K. Tobin, E. Grisan, P. Favaro, A. Ruggeri, and E. Chaum, "Textureless macula swelling detection with multiple retinal fundus images," IEEE Trans. Biomed. Eng., vol. 58, no. 3, pp. 795–799, Mar. 2011.
- [3] M. R. Hee, C. A. Puliafito, C. Wong, J. S. Duker, E. Reichel, B. Rutledge, J. S. Schuman, E. A. Swanson, and J. G. Fujimoto, "Quantitative assessment of macular edema with optical coherence tomography," Arch. Ophthalmol., vol. 113, no. 8, pp. 1019–1029, Aug. 1995.
- [4] J. Davidson, T. Ciulla, J. McGill, K. Kles, and P. Anderson, "How the diabetic eye loses vision," Endocrine, vol. 32, pp. 107–116, Nov. 2007.
- [5] C. P. Wilkinson, F. L. Ferris, R. E. Klein, P. P. Lee, C. D. Agardh, M. Davis, D. Dills, A. Kampik, R. Pararajasegaram, and J. T. Verdaguer, "Proposed international clinical diabetic retinopathy and diabetic macular edema disease severity scales," Am. Acad. Ophthalmol., vol. 110, no. 9, pp. 1677–1682, Sep. 2003.
- [6] R. F. N. Silberman, K. Ahlrich, and L. Subramanian, "Case for automated detection of diabetic retinopathy," Proc. AAAI Artif. Intell. Development (AI-D'10), pp. 85–90, Mar. 2010.
- [7] M. Verma, R. Raman, and R. E. Mohan, "Application of tele ophthalmology in remote diagnosis and management of adnexal and orbital diseases," Indian J. Ophthalmol., vol. 57, no. 5, pp. 381–384, Jul. 2009.
- [8] M. D. Abramoff, M. Niemeijer, M. S. Suttorp-Schulten, M. A. Viergever, S. R. Russell, and B. van Ginneken, "Evaluation of a system for automatic detection of diabetic retinopathy from color fundus photographs in a large population of patients with diabetes," J. Diabetes Care, vol. 31, no. 2, pp. 193–198, Nov. 2007.
- [9] S. Philip, A. Fleming, K. Goatman, S. Fonseca, P. McNamee, G. Scotland, G. Prescott, P. F. Sharp, and J. Olson, "The efficacy of automated disease/no disease grading for diabetic retinopathy in a systematic screening programme," Br. J. Ophthalmol., vol. 91, no. 11, pp. 1512–7, Nov. 2007.
- [10] H. Jaafar, A. Nandi, and W. Al-Nuaimy, "Detection of exudates in retinal images using a pure splitting technique," in Proc. Annu. Int. Conf. IEEE Eng. Med. Biol. Soc. (EMBC), Aug. 2010, pp. 6745–6748.
- [11] P. C. Siddalingaswamy and K. G. Prabhu, "Automatic grading of diabetic maculopathy severity levels," in Int. Conf. Syst. Med. Biol.(ICSMB), Dec. 2010, pp. 331–334.
- [12] C. I. Sanchez, M. Garca, A. Mayo, M. I. Lopez, and R. Hornero, "Retinal image analysis based on mixture models to detect hard exudates," Med. Image Anal., vol. 13, no. 4, pp. 650–658, Aug. 2009.
- [13] A. Osareh, M. Mirmehdi, B. Thomas, and R. Markham, "Automated identification of diabetic retinal exudates in digital colour images," Br. J. Ophthalmol., vol. 87, pp. 1220–1223, Oct. 2003.
- [14] T. Walter, J.-C. Klein, P. Massin, and A. Erginay, "A contribution of image processing to the diagnosis of diabetic retinopathy-detection of exudates in color fundus images of the human retina," IEEE Trans. Med. Imag., vol. 21, no. 10, pp. 1236–1243, Oct. 2002.
- [15] H. Wang, W. Hsu, K. G. Goh, and M. L. Lee, "An effective approach to detect lesions in color retinal images," in Proc. IEEE Conf. Comput. Vis. Pattern

- Recognit., 2000, vol. 2, pp. 181–186.
- [16] W. Hsu, P. Pallawala, M. L. Lee, and K.-G. A. Eong, “The role of domain knowledge in the detection of retinal hard exudates,” in Proc. 2001 IEEE Comput. Soc. Conf. Comput. Vis. Pattern Recognit. (CVPR2001), 2001, vol. 2, pp. II-246–II-251.
- [17] C. Sanchez, A. Mayo, M. Garcia, M. Lopez, and R. Hornero, “Automatic image processing algorithm to detect hard exudates based on mixture models,” in Proc. 28th Annu. Int. Conf. IEEE Eng. Med. Biol. Soc., Sep. 2006, pp. 4453–4456.
- [18] Y. Hatanaka, T. Nakagawa, Y. Hayashi, Y. Mizukusa, A. Fujita, M. Kakogawa, K. K.M. D., T. Hara, and H. Fujita, “Cad scheme to detect hemorrhages and exudates in ocular fundus images,” in Proc. SPIE Med. Imag. 2007: Comput.-Aided Diagn., Mar. 2007, vol. 6514, pp. 2M1–2M8.
- [19] S. Ravishankar, A. Jain, and A. Mittal, “Automated feature extraction for early detection of diabetic retinopathy in fundus images,” in IEEE Conf. Comput. Vis. Pattern Recognit., Jun. 2009, pp. 210–217.
- [20] A. Osareh, B. Shadgar, and R. Markham, “A computational-intelligence-based approach for detection of exudates in diabetic retinopathimages,” IEEE Trans. Inf. Technol. Biomed., vol. 13, no. 4, pp. 535–545, Jul. 2009.
- [21] H. Li and O. Chutatape, “A model-based approach for automated feature extraction in fundus images,” in Proc. 9th IEEE Int. Conf. Comput. Vis., Oct. 2003, vol. 1, pp. 394–399.
- [22] M. Garcia, R. Hornero, C. Sanchez, M. Lopez, and A. Diez, “Feature extraction and selection for the automatic detection of hard exudates in retinal images,” in Proc. 29th Annu. Int. Conf. IEEE Eng. Med. Biol. Soc., Aug. 2007, pp. 4969–4972.
- [23] K. Ram and J. Sivaswamy, “Multi-space clustering for segmentation of exudates in retinal color photographs,” in Proc. Annu. Int. Conf. IEEE Eng. Med. Biol. Soc., Sep. 2009, pp. 1437–1440.
- [24] A. Rocha, T. Carvalho, S. Goldenstein, and J. Wainer, “Points of interest and visual dictionary for retina pathology detection Inst. Comput., Univ. Campinas, Tech. Rep. IC-11-07, Mar. 2011.
- [25] C. Agurto, V. Murray, E. Barriga, S. Murillo, M. Pattichis, H. Davis, S. Russell, M. Abramoff, and P. Soliz, “Multiscale am-fm methods for diabetic retinopathy lesion detection,” IEEE Trans. Med. Imag., vol. 29, no. 2, pp. 502–512, Feb. 2010.
- [26] N. P. Ward, S. Tomlinson, and C. J. Taylor, “Image analysis of fundus photographs. the detection and measurement of exudates associated with diabetic retinopathy,” Ophthalmology, vol. 96, no. 1, p. 86-6, Jan. 1989.
- [27] W. Huan, H. Wynne, and L. M. Li, “Effective detection of retinal exudates in fundus images,” in Proc. 2nd Int. Conf. Biomed. Eng. Informat., Oct. 2009, pp. 1–5.
- [28] J. Singh, G. D. Joshi, and J. Sivaswamy, “Appearance-based object detection in colour retinal images,” in Proc. Int. Conf. Image Process., 2008, pp. 1432–1435.
- [29] G. D. Joshi, J. Sivaswamy, K. Karan, and S. R. Krishnadas, “Optic disk and cup boundary detection using regional information,” in Proc. Int. Conf. Image Process., 2010, pp. 948–951.
- [30] J. V. Stone, “Object recognition using spatiotemporal signatures,” Vision Research, vol. 38, no. 7, pp. 947–951, Apr. 1998.



Shobhana.M received B.tech degree in Electronics and communication Engineering from Calicut University in 2010. She is pursuing Master of Engineering in Applied Electronics at K.S.R College of Engineering. She presented a paper in an International conference at Karunya University. Her research interest includes medical imaging, retinal imaging and application of digital image processing in medical images.



S.B.Chitrapreyanka received B.E degree in Electronics and Communication Engineering from Bharathiar University, Coimbatore in 1997. She received M.E degree in Power Electronics and Drives from Anna University, Chennai in May 2007. Currently working as assistant professor in K.S.R College of Engineering. Her area of interest includes Power Electronics Converter, Digital Controller based Drives.